Supplemental Material to the article

"Superconductivity suppression in disordered films: Interplay of two-dimensional diffusion and three-dimensional ballistics"

In this Supplemental material we discuss several technical details, which are left unexplained in the main text of the Letter.

A. Cooper susceptibility and the critical temperature. The starting point of our analysis is the zero-momentum Cooper susceptibility [45]:

$$L = \int d\mathbf{r} \int^{1/T} d\tau \left\langle \psi_\downarrow^+(\mathbf{r},\tau)\psi_\uparrow^+(\mathbf{r},\tau)\psi_\uparrow(0,0)\psi_\downarrow(0,0)\right\rangle. \tag{S1}$$

The divergence of L as a function of temperature T marks the transition to the superconducting state.

The basic element of the theory is the disorder-averaged Matsubara Green function

$$G_{\pm E}(\mathbf{k}) = \frac{1}{\pm iE - \xi_\mathbf{k} \pm i/2\tau}. \tag{S2}$$

For calculations in the momentum representation, we use the approximation $\xi_\mathbf{k} = v_F\left(|\mathbf{k}| - k_F\right)$, which breaks down in the vicinity of the Fermi momentum. When working in the real space, we assume a parabolic dispersion of the electron spectrum: $\xi_\mathbf{k} = k^2/2m - E_F$.

In order to calculate L, we need to draw all possible diagrams with the interaction vertices $\lambda_{\rm ph}$ and λ, and average them over disorder. It is convenient to calculate ladders of repulsive interaction lines λ first and then insert the corresponding block (denoted as Π) between the attractive phonon lines $\lambda_{\rm ph}$. Summing the corresponding ladder, we obtain

$$L = \frac{\Pi}{1 - \lambda_{\rm ph}\Pi/\nu}. \tag{S3}$$

As the block Π is inserted between the phonon lines, energy cutoff at the Debye frequency ω_D is implied at its edges. Equation (S3) allows to express the critical temperature in terms of Π through the relation

$$\nu\lambda_{\rm ph}^{-1} = \Pi(T_c). \tag{S4}$$

B. Ballistic disorder ladders. In the following calculation we will need the expression for the "ballistic" cooperon and diffuson $\mathcal{C}(\mathbf{q},\omega)$ derived at arbitrary values of ql, $\omega\tau$ (but we still assume that $q \ll k_F$ and $\omega \ll E_F$). Taking $E > 0$ and $E - \omega < 0$, we get for one step of the ladder [68]:

$$f_q(\omega) = \frac{\nu}{2\pi\nu\tau}\int\frac{d\Omega}{4\pi}\int d\xi\,\frac{1}{iE - \xi + i/2\tau}\frac{1}{i(E-\omega) - \xi - \boldsymbol{v}\boldsymbol{q} - i/2\tau} = \frac{1}{ql}\arctan\frac{ql}{1+\omega\tau}. \tag{S5}$$

Summing the geometric series of the diffusive ladder, we obtain

$$\mathcal{C}(\mathbf{q},\omega) = \frac{1}{2\pi\nu\tau}\frac{1}{1 - f_q\left(\omega\right)}; \qquad \mathcal{C}(0,\omega) = \frac{1}{2\pi\nu\tau}\frac{1+\omega\tau}{\omega\tau}. \tag{S6}$$

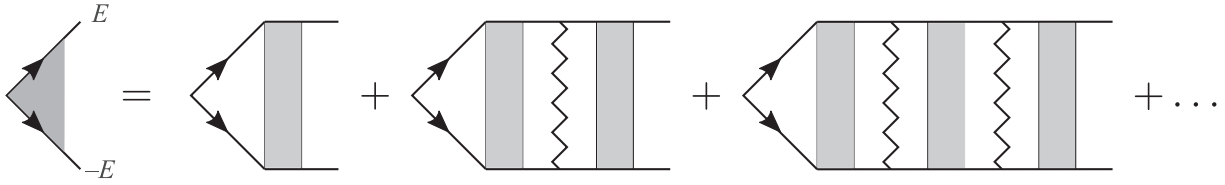

Fig. S1. Diagrammatic equation for the renormalized Cooper vertex $v(E)$. Zigzag lines stand for the repulsive interaction λ. Blocks with no impurity lines between the interaction lines are also included. The outer Green functions are not included into the expression for $v(E)$

C. Renormalization of the phonon vertex. In order to deal with logarithmic contributions originating from various energy intervals, it is convenient to introduce the renormalized phonon vertex $\upsilon(E)$ defined as the sum of the sequence of diagrams shown in Fig. S1. In brief, $\upsilon(E)$ takes into account ladders of the interaction lines (repulsion constant λ), which are known to be responsible for the "Tolmachev logarithm" (Morel–Anderson pseudopotential) renormalisation [61–63]. In the quasiballistic region it is important to account for the diagrams, where the diffusive ladder may be absent (no impurity lines). Since the vertex contains the photon interaction, the energy arguments in the pair of Green functions adjacent to the vertex should be smaller than ω_D. This property is taken into account by introducing the step function $\theta(\omega_D - |E|)$ to the first term of the series and restricting integrations over internal energies in the other terms (see below). The renormalised phonon vertex then takes the form

$$\upsilon(E) = \left[1 + \frac{2\pi\nu\tau}{1+2|E|\tau}\mathcal{C}(0, 2|E|)\right] u(E) = \frac{1+2E\tau}{2E\tau}u(E), \tag{S7}$$

where

$$u(E) = \theta(\omega_D - |E|) - \frac{\lambda}{\nu}T\sum_{E'}^{\omega_D}\frac{\pi\nu}{E'} + \left(-\frac{\lambda}{\nu}\right)^2 T^2 \sum_{E'}^{\omega_D}\frac{\pi\nu}{E'}\sum_{E''}^{E_F}\frac{\pi\nu}{E''} + \cdots = \theta(\omega_D - |E|) - \frac{\lambda\log\omega_D/T}{1+\lambda\log E_F/T}. \tag{S8}$$

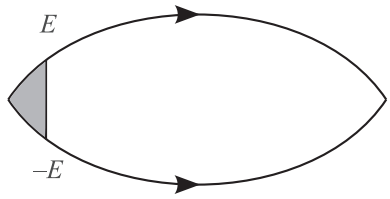

Fig. 2. Cooper bubble Π_0 in the no-crossing approximation

D. Anderson theorem. In the leading no-crossing approximation, Π is given by the diagram depicted in the Fig. S2 and equals

$$\Pi_0(T) = 2\pi\nu\tau\sum_{E}^{\omega_D} f_0(2|E|)\upsilon(E) = \nu\frac{1+\lambda\log E_F/\omega_D}{1+\lambda\log E_F/T}\log\frac{\omega_D}{T}. \tag{S9}$$

This expression appears to be disorder-independent, which leads to the insensitivity of the critical temperature to potential disorder in the leading order (Anderson theorem) [64–66]. Solving Eq. (S4) with $\Pi = \Pi_0$, we get the standard Bardeen–Cooper–Schrieffer (BCS) expression (5) with the renormalised coupling constant λ_{BCS} given by Eq. (6).

E. Crossing corrections to $\Pi(T)$. Contributions to Π beyond the non-crossing approximation are responsible for the shift of T_c. Assuming that $\delta\Pi$ is small and linearizing Eq. (S4), we get the following equation for δT_c in the first order:

$$\nu\lambda_{\mathrm{ph}}^{-1} = \Pi_0(T_{c0} + \delta T_c) + \delta\Pi(T_{c0}). \tag{S10}$$

Hence we get for the perturbative shift of T_c:

$$\frac{\delta T_c}{T_{c0}} = \frac{\delta\Pi}{\nu}\left(\frac{1+\lambda\log E_F/T_{c0}}{1+\lambda\log E_F/\omega_D}\right)^2 = \frac{\delta\Pi}{\nu}\left(\frac{\lambda_{\mathrm{ph}}}{\lambda_{\mathrm{BCS}}}\right)^2. \tag{S11}$$

In general, account for the renormalisation effects can be done with the help of Eq. (S11) and insertion of renormalised Cooper vertices $\upsilon(E)$ into the ends of the diagrams, which describe the correction to the Cooper bubble, $\delta\Pi$. This procedure leads to Eqs. (7) and (15).

Applying this technique to the ballistic vertex correction reproduces the result obtained in the Letter by interpreting this correction as a shift of the bare Cooper-channel constant $\delta\lambda^c$ and expanding Eqs. (5) and (6). On the other hand, applying the same technique to corrections originating at energies $E < \omega_D$ (as the main part of the 2D diffusive Finkel'stein–Ovchinnikov correction) leads to the cancellation of the renormalisation factors.

F. Momentum-space calculation of the critical temperature shift. Below we sketch the derivation of Eqs. (7) and (8), which represent the contribution of inelastic diagrams (depicted in Fig. 2) to the T_c shift. The

calculation is done in the momentum representation in terms of ballistic diffusons and cooperons [see Eq. (S6)] to assess the crossover to the ballistic region.

The first diagram in Fig. 2 represents a correction $\delta\Pi_a$ to be inserted between the phonon lines in the Cooper ladder. When substituted to Eq. (S11) it results in Eq. (7) with

$$I^{(a)}_{E,E'} = \frac{\tau}{d}\sum_{q_z}\int \frac{d\mathbf{q}_\parallel}{(2\pi)^2}\frac{f_q(E+E')^2}{1-f_q(E+E')}, \tag{S12}$$

where Eqs. (S5) and (S6) were used and summation over diffusive modes in the film geometry is implied [to be replaced by usual 3D integration $\int(d^3\mathbf{q})$ when studying crossover from 3D diffusion to 3D ballistics]. The numerator in Eq. (S12) represents two triangular Hikami boxes in the diagram, while the denominator corresponds to the Cooperon ladder.

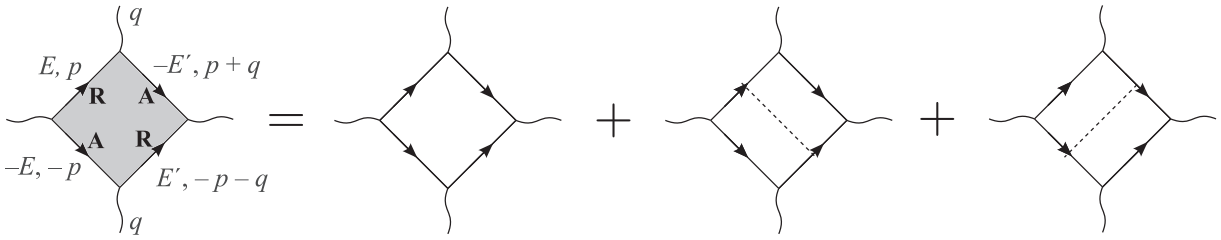

Fig. S3. Hikami box $H(q, E, E')$ made of four Green functions

Calculation of the second diagram in Fig. 2 involves computation of the ballistic Hikami box made of of four Green functions (see Fig. S3), which is given by

$$H(q,E,E') = 4\pi\nu\tau^3\frac{f_q(E+E')[1-f_q(E+E')]}{(1+2E\tau)(1+2E'\tau)}. \tag{S13}$$

Then the contribution of the second diagram is given by Eq. (7) with

$$I^{(b)}_{E,E'} = \frac{\tau}{d}\sum_{q_z}\int \frac{d\mathbf{q}_\parallel}{(2\pi)^2}\frac{f_q(E+E')^3[1-f_q(E+E')]}{[1-f_q(E+E')]^2}, \tag{S14}$$

where the denominator originates from two diffusons in the central part of the diagram and the numerator is the Hikami box (S13) multiplied by two additional $f_q(E+E')$ factors, stemming from the integrals of the "bubbles" $G_E(p)G_{-E'}(p+q)$ and $G_{-E}(p')G_{E'}(p'-q)$.

Finally, in order to be able to trace a crossover to the ballistic region, one should also include the diagram obtained from the second diagram in Fig. 2 by leaving only one out of the two diffusons encircling the interaction line. That leads to Eq. (7) with

$$I^{(b')}_{E,E'} = 2\frac{\tau}{d}\sum_{q_z}\int \frac{d\mathbf{q}_\parallel}{(2\pi)^2}\frac{f_q(E+E')^2[1-f_q(E+E')]}{1-f_q(E+E')}. \tag{S15}$$

Finally, summing Eqs. (S12), (S14), and (S15), one arrives at Eq. (8).

G. Elastic diagrams. The central part $\delta P^{\rm elastic}$ of elastic diagrams is depicted in Fig. S4, where we work in terms of the exact eigenstates (labeled by a, a') of the Hamiltonian in the presence of disorder. The corresponding analytical expression is:

$$\delta P^{\rm elastic} = T^2\sum_{E,E'}\sum_{a,a'} V_{aa'}G_a(E)G_a(-E)\left[G_a(E)+G_a(-E)\right]G_{a'}(E'), \tag{S16}$$

where the matrix element of the interaction $V_{aa'} = -(1-s)(\lambda/\nu)\int d\mathbf{r}\,|\phi_a(\mathbf{r})|^2|\phi_{a'}(\mathbf{r})|^2$ includes both Fock (exchange) and Hartree terms (with spin degeneracy factor $s=2$ in the latter). Here $\phi_a(\mathbf{r})$ are the wavefunctions corresponding to the energies ξ_a. The Matsubara Green function in this representation is $G_a(E) = 1/(iE-\xi_a)$. After some algebra, Eq. (S16) can be rewritten [42] in the form

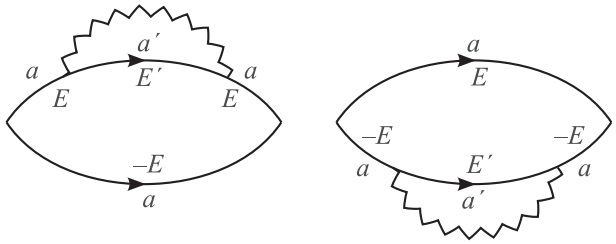

Fig. S4. The central part of elastic diagrams to the Cooper susceptibility in the exact-eigenstates representation

$$\delta P^{\text{elastic}} = T^2 \sum_E \frac{1}{2iE} \sum_{E'} \sum_{aa'} V_{aa'} \left[G_a^2(E) - G_a^2(-E) \right] G_{a'}(E'), \tag{S17}$$

where one recognises corrections to the Green functions at coincident points (δG_E and δG_{-E}) summed over Matsubara energies with a factor $T/(2iE)$. Adding renormalised vertices $\upsilon(E)$ [Eq. (S7)] and substituting to Eq. (S11), one arrives at the expression

$$\frac{\delta T_c^{\text{elastic}}}{T_c} = \left(\frac{\lambda_{\text{ph}}}{\lambda_{\text{BCS}}} \right)^2 iT \sum_{E=E_n} \frac{u(E)^2}{E} \frac{\delta G_E - \delta G_{-E}}{\nu_0}. \tag{S18}$$

Now using the analyticity property, which relates the Matsubara Green function with the real-time retarded Green function G^R (at coinciding points in our case),

$$G_E = \frac{1}{\pi} \int d\varepsilon \, \frac{\operatorname{Im} G^R(\varepsilon)}{\varepsilon - iE} = - \int d\varepsilon \, \frac{\nu(\varepsilon)}{\varepsilon - iE}, \tag{S19}$$

one can finally express [40] the result for the contribution of elastic diagrams to the T_c shift via the correction to the tunneling density of states, arriving at Eq. (15) of the main text.